Interspecies Sequence Variations Affect the Kinetics and Thermodynamics of Amyloid Formation: Peptide Models of Pancreatic Amyloid

Ted T. Ashburn and Peter T. Lansbury, Jr.*

Department of Chemistry
Massachusetts Institute of Technology
Cambridge, Massachusetts 02139

Human pancreatic amyloid deposits comprising the islet amyloid polypeptide (IAPP[H], Figure 1) are characteristic of type II diabetes.[1] A 10 amino acid sequence within IAPP[H] (residues 20–29) is sufficient for amyloid formation.[2,3] We proposed a model for the IAPP[H](20–29) peptide amyloid based on electron microscopy (EM),[3] Fourier-transform infrared spectroscopy (FTIR), and solid-state nuclear magnetic resonance spectroscopy (ssNMR) studies,[4] in which the GAIL[5] sequence (residues 24–27) forms an ordered antiparallel β-sheet, while the termini of the peptide have a less regular and possibly more flexible structure.[4] A peptide based on the rat IAPP(20–29) sequence, which differs from IAPP[H] at positions 23, 25, 26, 28, and 29, is not amyloidogenic.[6] However, a peptide based on the cat IAPP sequence (IAPP[C](20–29), Figure 1), which differs from the human sequence at positions 23 (Leu vs Phe) and 29 (Pro vs Ser), forms amyloid fibrils *in vitro*.[3,7] We report herein that both of these changes decrease the rate of nucleation and the rate of growth of the fibril and increase the solubility of the amyloid fibril.

To *separately* measure the effects of the two amino acid differences between the human and cat IAPP(20–29) sequences, two peptides, in which each change was introduced separately (IAPP[H](20–29)F23L and IAPP[H](20–29)S29P, Figure 1), were studied, in addition to peptides based on the human (IAPP[H](20–29)) and cat (IAPP[C](20–29)) sequences.[8] These four peptides constitute a cycle, the characteristics of which provide information regarding the structural basis of amyloid formation. If residues 23 and 29 do not interact in the fibril, then the kinetic and thermodynamic effects of each individual "mutation" would be expected to additive (ln(F23L) + ln(S29P) = ln(overall effect), Figure 1).[9,10] In such a case, the effects of each "mutation" would
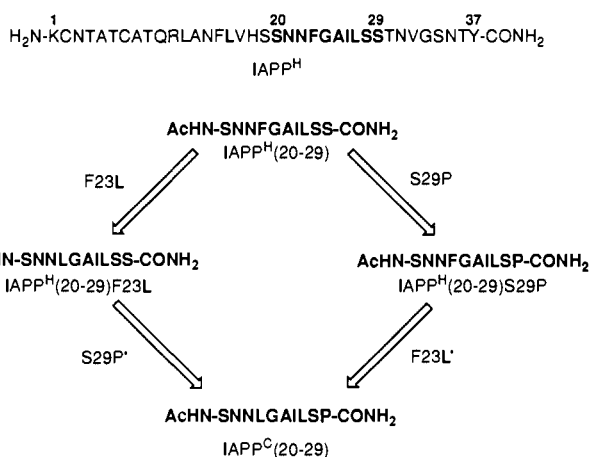

Figure 1. Primary structure of IAPP[H] and the cycle created by the four peptides discussed in this paper.[10]

be context-independent (i.e., S29P = S29P' and F23L = F23L') and the cycle would be rectangular. Alternatively, if residues 23 and 29 do interact, then the individual effects would be nonadditive (ln(F23L) + ln(S29P) ≠ ln(overall effect)) and context-dependent (e.g., S29P ≠ S29P').[10]

Each peptide slowly formed amyloid fibrils (EM) from a supersaturated solution.[11] The resultant fibrils produced indistinguishable FTIR spectra, suggestive of antiparallel β-sheet structure (maximum at *ca.* 1630 cm^{-1}).[12,13] Peptide films,[4] formed by rapid evaporation of formic acid solutions, produced FTIR spectra similar to those of the fibrils, with one exception: the IAPP[C](20–29) film FTIR spectrum indicated disordered structure (broad absorption band centered at 1641 cm^{-1}). This result suggested that amyloid formation was slowest for the cat sequence and inspired the kinetic studies discussed below.

Amyloid formation is a nucleation-dependent process.[13–16] The requirement for nucleation leads to a delay in the appearance of insoluble amyloid fibrils, or lag time (Figure 2). The duration of the lag time depends, in part, on the association equilibria leading to nucleus formation (K_n).[17] Each single amino acid change resulted in a *ca.* 3-fold increase in the lag time relative to IAPP[H](20–29) (F23L = 2.7-fold, S29P = 3.6-fold; Table I), while the IAPP[C](20–29) peptide nucleated approximately 13-

(1) Nishi, M.; Sanke, T.; Nagamatsu, S.; Bell, G. I.; Steiner, D. F. *J. Biol. Chem.* **1990**, *265*, 4173.

(2) Glenner, G. G.; Eanes, D.; Wiley, C. *Biochem. Biophys. Res. Commun.* **1988**, *155*, 608.

(3) Westermark, P.; Engstrom, U.; Johnson, K. H.; Westermark, G. T.; Betsholtz, C. *Proc. Natl. Acad. Sci. U.S.A.* **1990**, *87*, 5036.

(4) Ashburn, T. T.; Auger, M.; Lansbury, P. T., Jr. *J. Am. Chem. Soc.* **1992**, *114*, 790.

(5) One letter amino acid codes: A = Ala, C = Cys, F = Phe, G = Gly, H = His, I = Ile, K = Lys, N = Asn, P = Pro, Q = Gln, R = Arg, S = Ser, T = Thr, V = Val, Y = Tyr.

(6) Rats do not develop pancreatic amyloid or type II diabetes.[21] IAPP[R](20–29) (AcHN-SNNLGPVLPP-CONH$_2$) does not form amyloid fibrils (solubility = 60 500 ± 3800 μM). Cats develop pancreatic amyloid in conjunction with type II diabetes.[7]

(7) Betsholtz, C.; Christmanson, L.; Engstrom, U.; Rorsman, F.; Jordan, K.; O'Brien, T. D.; Murtaugh, M.; Johnson, K. H.; Westermark, P. *Diabetes* **1990**, *39*, 118.

(8) Syntheses were performed using 9-fluorenylmethoxycarbonyl (Fmoc) amine protection and benzotriazol-1-yl-oxytris(pyrrolidino)phosphonium hexafluorophosphate (PyBOP) couplings. The Rink amide ((4-(2',4'-dimethoxyphenyl)(Fmoc)aminomethylphenyl)oxy)acetamidonorleucyl–MBHA resin (Novabiochem) provided the C-terminal amide, and the N-terminus was acetylated with acetic anhydride. Serine (*tert*-butyl) and asparagine (trityl) were deprotected and the peptides cleaved from the resin according to a published procedure.[22] Peptides were purified by isocratic reversed-phase high-pressure liquid chromatography (RPHPLC) on a YMC C18 column (300-Å pore size, 15-μm particle size, 30 × 300 mm²). Purity of each peptide was judged to be >98% by isocratic analytical RPHPLC (Waters C4 column (300-Å, 3.9 × 30 mm²)). Each peptide had an amino acid composition and plasma desorption mass spectrum consistent with the proposed primary structure.

(9) Perry, K. M.; Onuffer, J. J.; Gittelman, M. S.; Barmat, L.; Matthews, C. R. *Biochemistry* **1989**, *28*, 7961.

(10) Ackers, G. K.; Smith, F. R. *Annu. Rev. Biochem.* **1985**, *54*, 597.

(11) Peptide aggregation was initiated by adding a solution of the peptide (100 μL, 6.9 mM in DMSO by amino acid analysis (aaa)) to 900 μL of pH 7.4 buffer (100 mM NaCl, 1.8 mM NaH$_2$PO$_4$, 8.2 mM Na$_2$HPO$_4$, 0.2% NaN$_3$) in a 10- × 75-mm² disposable culture tube at room temperature. Samples were stirred at ~1550 rpm with a 3- × 10-mm² magnetic stirring bar. Turbidity was measured at 400 nm vs buffer. Thermodynamic solubility was determined after the aggregated solutions were stirred for 1 week. The samples were then centrifuged for 25 min at 2100g, the supernatants were filtered through Millex-GV 0.22-μm aqueous filters (Millipore), and peptide concentrations were determined by aaa.

(12) Krimm, S.; Bandekar, R. J.; *Adv. Prot. Chem.* **1986**, *38*, 181.

(13) Jarrett, J. T.; Lansbury, P. T., Jr. *Biochemistry* **1992**, *31*, 12345.

(14) Come, J. H.; Fraser, P. E.; Lansbury, P. T., Jr. *Proc. Natl. Acad. Sci. U.S.A.* **1993**, *90*, 5959.

(15) Jarrett, J. T.; Berger, E. P.; Lansbury, P. T., Jr. *Biochemistry* **1993**, *32*, 4693.

(16) Jarrett, J. T.; Lansbury, P. T., Jr. *Cell* **1993**, *73*, 1.

(17) For the simplest aggregation mechanism, where the nucleus is assembled by successive addition of monomers, the lag time is exponentially dependent on the number of monomers required to form the nucleus.[16] The aggregation experiments reported herein were done with consistent stirring, due to the need to suspend the aggregate to accurately measure turbidity.[11] We have observed that stirring greatly increases the nucleation rate. In the case of IAPP[H](20–29), the reaction order in peptide was determined to be between 1 and 2. In an unstirred case, where the reaction order could be much greater, small changes in K_n (which may correspond to similar changes in K_s) will have dramatic effects on the lag time.[15,16] Stirring may change the mechanism of amyloid formation by increasing the diffusion of small oligomers or by breaking up small fibrils to increase the number of growth faces.

Table I

peptide	lag time[a] (factorial increase relative to IAPP^H(20–29)), s	thermodynamic solubility[b] (factorial increase), μM	growth rate × 10^4 [c] (factorial decrease), ΔO.D.·s^{-1}	IAPP^H(20–29) seeded lag time,[d] s
IAPP^H(20–29)	310	9.0	25	26
IAPP^H(20–29)F23L	840 (2.7)	14 (1.6)	5.8 (4.3)	127
IAPP^H(20–29)S29P	1100 (3.6)	32 (3.6)	4.2 (6.0)	126
IAPP^C(20–29)	4000 (13)	109 (12)	1.0 (25)	171

[a] Lag time observed for each peptide at 690 μM. Each value is an average of at least three separate experiments and was determined by solving for the best fit line to the growth phase of the aggregation curve for $y = 0$. The error in these measurements was <25% for IAPP^H(20–29) and IAPP^C(20–29) and <10% for the "mutants" (F23L, S29P). [b] Thermodynamic solubility of each peptide. Each value is an average of three separate experiments. The error in these measurements was *ca.* 10% for IAPP^H(20–29) and IAPP^H(20–29)F23L and <10% for the more soluble peptides. [c] Amyloid fibril growth rate of each peptide ($\alpha K_g/k_{off}$). Turbidity (O.D.) was measured at 400 nm. Each value is an average of at least three experiments and was determined from the slope of the best fit line to the growth phase of the aggregation curve (Figure 2). The error in these values was <30% for the IAPP^C(20–29) and <15% for the other peptides. [d] Lag time of IAPP^H(20–29) at 690 μM after the addition of 10 mol % of peptide fibrils (seeds). Each value is an average of two separate experiments and was determined by solving for the best fit line to the growth phase of the aggregation curve (Figure 2) for y = initial turbidity (400 nm). The error in the short lag time (IAPP^H(20–29)) was *ca.* 40%; however, the error in the other measurements was <8%.
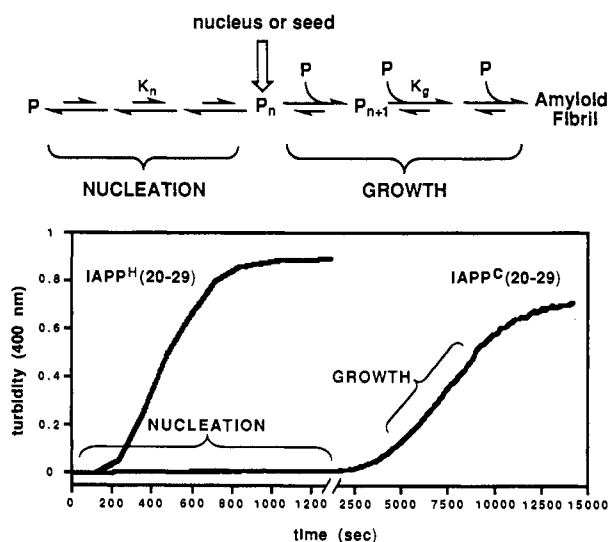

Figure 2. (Top) Simple mechanism for amyloid fibril formation.[16] (Bottom) Representative aggregation curves for IAPP^H(20–29) and IAPP^C(20–29) at 690 μM measured by turbidity (400 nm).[11] Note the discontinuous scale on the x axis.

fold more slowly than IAPP^H(20–29). Due to experimental error, it is not possible to determine whether the effects of each mutation on nucleation are independent or coupled.

The postnucleation equilibrium constant (K_g, Figure 2) defines the thermodynamic solubility of each amyloid peptide (Table I). The F23L and S29P changes increased the solubility by 1.6-fold and 3.6-fold, respectively. Assuming independent effects, the IAPP^C(20–29) peptide was expected to be *ca.* 6-fold more soluble than IAPP^H(20–29) ($\Delta\Delta G$ = ln F23L + ln S29P). However, the IAPP^C(20–29) peptide was *ca.* 12-fold more soluble than IAPP^H(20–29). The coupling of the two effects indicates that residues 23 and 29 interact in the amyloid fibril. This interaction could be direct or indirect, intramolecular or intermolecular. An intramolecular interaction is unlikely, since the effects of the mutations on the growth rate and, possibly, the lag time are independent. Therefore, we propose a direct intermolecular interaction between the side chains of F23 and S29 in the IAPP^H(20–29) fibril. This proposal is consistent with our crude two-dimensional model of the IAPP^H(20–29) amyloid fibril.[4]

The low relative solubility of IAPP^H(20–29) amyloid derives, in part, from its relatively rapid rate of growth (Table I). The effects of the two mutations on growth rate appear to be independent, suggesting that the growth rate depends primarily on the solution properties of the peptide.

Structural differences between the four peptide fibrils were not detected by EM or FTIR but were suggested by seeding experiments. Amyloid formation can be seeded by preformed amyloid fibrils.[13–16] This templating effect is very sensitive to subtle differences in fibril structure which cannot be detected by standard methods.[13,14] The lag time of IAPP^H(20–29) can be essentially eliminated by the addition of IAPP^H(20–29) seed fibrils (Table I). IAPP^H(20–29)F23L and IAPP^H(20–29)S29P are less effective seeds for IAPP^H(20–29), and IAPP^C(20–29) is even less effective as a seed.[18] The observation that each of the peptide fibrils is a competent seed for IAPP^H(20–29) supports the critical nature of the shared GAIL region.[4]

Globular proteins can tolerate sequence changes without losing their ability to fold.[19] Similarly, many sequences are capable of forming amyloid fibrils.[3,20] However, subtle effects on the rate of amyloid formation or on the stability of the fibril may be critical factors in diseases which are characterized by *in vivo* amyloidogenesis.[16] We have shown herein that the conservative change from Phe to Leu at position 23 has a significant effect on the stability of the IAPP(20–29) amyloid fibril and on the rate of its formation. In addition, we have utilized an approach which is commonly used to study the *intra*molecular forces which govern the structure and folding of soluble, globular proteins[9,10] to probe the *inter*molecular forces which govern the structure and assembly of an insoluble amyloid protein. This approach allows the identification of the critical intermolecular interactions which drive amyloid formation.

(18) Attempted seeding with the amyloid peptide β34–42[23,24] was unsuccessful.

(19) Lim, W. A.; Sauer, R. T. *Nature* **1989**, *339*, 31.

(20) Lansbury, P. T., Jr. *Biochemistry* **1992**, *31*, 6865.

(21) Betsholtz, C.; Christmansson, L.; Engstrom, U.; Rosman, F.; Svensson, V.; Johnson, K. H.; Westermark, P. *FEBS Lett.* **1989**, *251*, 261.

(22) King, D. S.; Fields, C. G.; Fields, G. B. *Int. J. Pept. Protein Res.* **1990**, *36*, 255.

(23) Halverson, K.; Fraser, P. E.; Kirschner, D. A.; Lansbury, P. T., Jr. *Biochemistry* **1990**, *29*, 2639.

(24) Spencer, R. G. S.; Halverson, K. H.; Auger, M.; McDermott, A. E.; Griffin, R. G.; Lansbury, P. T., Jr. *Biochemistry* **1991**, *30*, 10382.